PHYSICAL REVIEW B VOLUME 36, NUMBER 1 1 JULY 1987

Antiferromagnetic correlations in almost-localized Fermi liquids

C. Gros, R. Joynt,* and T. M. Rice
Institut für Theoretische Physik, ETH-Zürich, CH-8093 Zürich, Switzerland
(Received 3 November 1986)

A Monte Carlo method is used to calculate various properties of one-band Gutzwiller wave functions which are formed by restricting the charge fluctuations in noninteracting wave functions. Gutzwiller's approximate formula for the kinetic energy is tested both for the ground state and excited states. The ground state is found to have strong antiferromagnetic short-range spin-spin correlations for nearly-half-filled bands, thus extending previous work on the half-filled case. These correlations are very sensitive to the choice of occupied Bloch states and when the occupation is distributed uniformly over the band they disappear. From this fact we conclude that correlations are present only at temperatures low compared to the coherence temperature. In the almost-localized limit it is advantageous to describe the system by an effective Hamiltonian which separates into a term due to the kinetic energy of the charge carriers and one due to the Heisenberg spin-spin coupling. We show that the almost-localized Fermi liquid can gain energy from both terms in the effective Hamiltonian. In other words the restrictions on charge fluctuations can cause spin correlations which in turn can stabilize the Fermi-liquid ground state.

I. INTRODUCTION

The study of heavy Fermi liquids has been a very active problem in recent years.[1] In these systems there is a strong on-site repulsion which restricts the number of fermions on a given site; nonetheless, these systems are not localized but Fermi liquids. The strong on-site correlations that result in the Fermi liquid cannot be treated in perturbation theory. Gutzwiller[2] proposed to study such systems by means of a wave function in which a projection operator P that restricts the numbers of fermions on any given site operates on a free-fermion wave function. The key question is how to treat the projection operator when calculating, for example, the kinetic energy. In his original work Gutzwiller[2] proposed an approximate formula (GAF) and since then his original derivation of this formula has been extended and simplified.[1(c)]

Another approach to this problem has been to introduce an auxiliary boson field to enforce the correlations. This so-called "slave"-boson technique was originally introduced for the single-site Kondo problem[3-5] and has now been widely used for the periodic Anderson-lattice Hamiltonian as well.[6-8] The relation between these two techniques has been clarified by Kotliar and Ruckenstein.[9] They showed that the GAF corresponds to a particular slave-boson mean-field theory in which several auxiliary boson fields are introduced to enforce the correlation-induced constraints. In the limit that the degeneracy (orbital plus spin) N_f of the local state on each site approaches ∞, there is no difference between the results using GAF (Ref. 10) and the slave boson and other approaches.[11-13,1(a)] The GAF, however, is also correct in the limit $N_f \rightarrow 1$ and in the weak-coupling limit when the on-site Coulomb interaction $U \rightarrow 0$. Thus it can be regarded as an interpolation scheme and, as Kotliar and Ruckenstein[9] showed, if one wishes to have a mean-field theory which correctly gives these limits one is led to this form. Of course, a correct interpolation does not mean that the values are correct for finite values of N_f and U. One can also do a systematic expansion about the $N_f, U \rightarrow \infty$ limit. An expansion in N_f^{-1}, to obtain the leading correction, has recently been carried through for the periodic Anderson model by Millis and Lee[14] and by Auerbach and Levin.[14]

It is possible to directly numerically evaluate the required expectation values of the projected wave function. These values can then be compared with the GAF. Such numerical calculations have been done for the half-filled case for finite chains up to 18 sites by Kaplan, Horsch, and Fulde.[15] Horsch and Kaplan[16] were the first to realize that such numerical evaluations can be done for finite systems in one and two dimensions using a Monte Carlo (MC) technique. They studied the spin-spin correlation function of a Gutzwiller wave function for a single-band half-filled Hubbard model in the large-U limit. In their original work they reported results for one-dimensional (1D) systems, but they have also studied 2D systems.[16(b)] The aim of this paper is to extend their studies to expectation values of other operators and to make a direct test of the GAF for the kinetic-energy operator and other operators. Recently, Shiba[17] has reported a series of Monte Carlo calculations on Gutzwiller-type wave functions for the periodic Anderson model in one dimension. He finds good agreement, in general, with the results obtained by Rice and Ueda[10] based on the GAF, at least if the f level is not too far into the Kondo regime. In that limit his numerical accuracy is more limited and direct comparisons are more difficult.

One remarkable result due to Kaplan, Horsch, and Fulde[15] is that the single-band (nondegenerate) Gutzwiller wave function in the $U \rightarrow \infty$, half-filled limit exhibits a remarkable degree of short-range magnetic order. In fact, their results show in one dimension a value for the expectation value $q_1 \equiv \langle s_i^z s_{i+1}^z \rangle$ indistinguishable from the exact result for the $s=\frac{1}{2}$ antiferromagnetic Heisenberg chain.

In two-dimensions the results of Horsch and Kaplan[16] on a square lattice also show strong short-range order, although in this case $|q_1|$ is significantly different than expected in the Heisenberg problem. Our results confirm their general conclusion. Due to a modification of their technique, we are able to study certain 1D states with a greatly improved size and number of Monte Carlo steps, with the result that we can see a very small but numerically significant difference between the 1D values of q_1 for the Gutzwiller wave functions and the exact Heisenberg values. We have extended the results to the case in which the number of particles per site, $n_f<1$, and have found, as expected, only a very small change in q_1. Our results for the kinetic energy as a function of $1-n_f$ give a value very close to the maximum obtainable value and one slightly higher than those given by the GAF for $N_f=2$. In general, we find that the GAF overestimates the gain in kinetic energy, but there are reasons to suspect that this is a consequence of the special band structure in one dimension and that the accuracy of the GAF improves in higher dimensions.

In discussing the effects of keeping U finite, Kaplan, Horsch, and Fulde[15] showed, for the Hubbard Hamiltonian, that it was favorable using the Gutzwiller wave function—to introduce a small density of doubly occupied sites d as soon as U is finite. This contradicts the conclusions of Brinkman and Rice[18] that $d\equiv 0$ for $U>U_c$ (U_c is the Mott-Hubbard critical value of U). There is, however, an alternative approach to finite U; namely, that one evaluates the energy with an effective Hamiltonian. Castellani *et al.* and Hirsch[19] have derived an effective Hamiltonian which clearly distinguishes the effect of a real promotion of electrons from the lower to upper Hubbard bands to give $d>0$ and a finite density of carriers, from the virtual hopping processes (which also make $d>0$ and cause an antiferromagnetic Heisenberg coupling). The former does not occur for large U and the latter, of course, do not give rise to free carriers. The Gutzwiller wave function gives an excellent energy for the Fermi-liquid state with $1-n_f>0$, U finite and large, if we use the effective Hamiltonian, since it has a very good kinetic energy for the holes and a very good value of q_1. It has the implication that the energy balance between localized and itinerant states is a subtle one, since there are strong short-range spin correlations in the Fermi liquids. Note that such short-range correlations were also found in the Anderson model by Shiba.[17] The unitary transformation from the Hubbard to the effective Hamiltonian amounts to a change of basis in the wave function, so that the use of an effective Hamiltonian with a Gutzwiller wave function is equivalent to using the original Hubbard Hamiltonian with a Gutzwiller wave function constructed from a transformed basis.

The spin-spin correlations have an important effect on the magnetic susceptibility. By explicit calculation we find that the antiferromagnetic correlations are reduced in an applied field and the Heisenberg coupling term in the effective Hamiltonian then generates a finite restoring force (i.e., a finite Curie-Weiss Θ). The kinetic-energy term is hardly changed, so that it is the Heisenberg-coupling term which determines the susceptibility. We have also examined these two questions; namely, the form of the spin-spin correlations and the accuracy of the GAF when an excited-state wave function is taken instead of the ground state. We find that the accuracy of the GAF is much reduced but the value of the kinetic energy remains higher in all the excited states that we examined. The strong antiferromagnetic spin-spin correlations that characterize the ground state are very sensitive to the choice of Bloch states that are occupied, and when the occupation probability is distributed over the band they disappear. From this we conclude that these antiferromagnetic spin correlations will be present only at temperatures that are low compared to the coherence temperature—an effect found in experiments on the heavy-electron metals.

This paper is organized as follows. In Sec. II we discuss the Monte Carlo method and introduce the modification which in one dimension greatly speeds up the Monte Carlo procedure. Then, in Sec. III the effective Hamiltonian in the large-U limit, but with a general value of N_f, is discussed. Note that we discuss the difference between the effective Hamiltonian appropriate to the Hubbard and Anderson models. The properties of the ground state, its energy, spin-spin correlations, and magnetic susceptibility are discussed in Sec. IV. Then, in Sec. V we examine a variety of excited states corresponding to changing the occupation probabilities in the Bloch-state part of the Gutzwiller wave function. Finally, we summarize our conclusions in Sec. VI.

II. METHODS

Throughout this paper we use the infinite-U Gutzwiller wave function

$$|\Psi_G\rangle=\prod_i(1-n_{i\uparrow}n_{i\downarrow})\prod_{k\,(<k_F),\sigma}c^\dagger_{k\sigma}|0\rangle=\sum_\alpha a_\alpha|\alpha\rangle\ , \qquad (1)$$

with $n_{i\uparrow}=c^\dagger_{i\uparrow}c_{i\downarrow}$. Our problem is to evaluate expectation values of the form

$$\langle\Psi_G|\theta|\Psi_G\rangle=\sum_{\alpha,\beta}a_\alpha a^*_\beta\theta_{\beta\alpha}\ . \qquad (2)$$

Here, α,β are states in which the electron spins have a definite spatial configuration. In other words, α is a label specifying the two disjoint sets $\{r\},\{r'\}$, which determine the positions of the up- and down-spin electrons, respectively. The corresponding coefficient a_α is proportional to the product of two Slater determinants with elements $\exp(ik_lr_m)$ and $\exp(ik_lr'_m)$, where l and m run from 1 to N_σ. N_σ is the total number of up ($\sigma=\uparrow$) or down ($\sigma=\downarrow$) electrons. We take a normalization $\sum_\alpha|a_\alpha|^2=1$. The choice of k values determines Ψ_G, which is defined on a line of L sites with periodic boundary conditions. Horsch and Kaplan[16(a)] were the first to recognize that this sort of expectation value is susceptible to a Monte Carlo (MC) evaluation. They applied this technique to the half-filled-band case for one, and in later work by Horsch and Kaplan,[16(b)] two dimensions. Recently, Shiba has implemented these methods for the infinite-U Gutzwiller wave function for the periodic Anderson model.[17] Since these authors have presented details of the method, we limit our discussion to a few points where our techniques differ from theirs.

Let us first consider the simplest case, where θ is diagonal, $\theta_{\beta\alpha}=0$ if $\alpha\neq\beta$. The most difficult part of the computation is $T(\alpha\to\alpha')$, the MC weighting factor in going from one configuration, α, to another, α'. This is given by the detailed-balance conditions

$$T(\alpha\to\alpha')=1, \quad |a_{\alpha'}|^2>|a_\alpha|^2 ,$$

and

$$T(\alpha\to\alpha')=|a_{\alpha'}|^2/|a_\alpha|^2 \quad \text{when } |a_\alpha|^2>|a_{\alpha'}|^2 .$$

$\theta_{\alpha\alpha}$ is then averaged over a sequence of states determined by the T's. α' is generated from α by the interchange of electrons with different spins, or the motion of an electron to an empty site. We follow Horsch and Kaplan[16(a)] and interchange only nearest-neighbor spins. In this case the MC weighting factors are multiplied by a configurational weighting factor which is straightforward to calculate. The rate-determining factor is the evaluation of the ratio of determinants $a_\alpha/a_{\alpha'}$. If this is done by the inverse-update method of Ceperley *et al.*,[20] then a number of multiplications of order N_σ^2 per spin degree of freedom is required. In one dimension, at least for certain states, this can be improved upon considerably. A determinant of a matrix with elements $\exp(ik_l r_m)$, where the k_l form an arithmetic progression, i.e., $k_l=k_0+l\Delta k$, $l=0,\ldots,N_\sigma-1$, is a Vandermonde determinant, it has the form

$$\begin{vmatrix} 1 & z_1 & z_1^2 & \cdots & z_1^{N_\sigma-1} \\ 1 & z_2 & z_2^2 & \cdots & \\ 1 & z_3 & & \cdots & \\ \vdots & & & & \\ 1 & & & \cdots & z_{N_\sigma}^{N_\sigma-1} \end{vmatrix} ,$$

where $z_l=\exp(i\Delta k r_l)$. This, in turn (by inspection of its zeros), is simply equal to

$$\prod_{\substack{l,m \\ (l<m)}} (z_l-z_m) .$$

A ratio of two such determinants is then

$$\prod_{\substack{m \\ (m\neq n)}} (z_n-z_m)/(z_n'-z_m) ,$$

when the position of only the n'th electron has been changed from r_n to r_n'. $|a_\alpha/a_{\alpha'}|^2$ is then the product of the square moduli of N_f such expressions. Note also that

$$|z_l-z_m|^2=4\sin^2\left[\Delta k\left[\frac{r_l-r_m}{2}\right]\right] , \tag{3}$$

so that no complex arithmetic is required. Therefore we have only of order N_σ operations. This allows us to treat much larger systems. The method is suitable for the ground state, since then $k_0=-k_F$ and $\Delta k=2\pi/L$. A certain class of excited states can also be investigated in this way.

It is interesting to note that the evaluation of expectation values in the Gutzwiller ground state can be mapped onto a statistical-mechanical problem. The statistical-mechanics model has positions evenly distributed on a ring. Unlike charges interact via a zero-range infinite repulsive interaction. There is a logarithmic interaction $V(r_i,r_j)=-2q^2\ln|z_i-z_j|$ between like charges. The square of the charge divided by the temperature is then set equal to $\frac{1}{2}$. This model is a generalization of a model which was exactly solved by Dyson.[21] However, his methods do not seem to generalize to the case at hand.

We are also interested in off-diagonal operators, e.g., the kinetic energy. To obtain these, we can rewrite (2) as

$$\langle\Psi_G|\theta|\Psi_G\rangle=\sum_\alpha |a_\alpha|^2\left[\sum_\beta \theta_{\beta\alpha}(a_\beta^*/a_\alpha^*)\right] . \tag{4}$$

We can then proceed as before, using precisely the same transition probabilities to generate the states, and measuring the quantity appearing in the large parentheses. Two things make the extension feasible. First, the measured quantity involves again a *ratio* of determinants of exactly the same kind as are needed for the transition probabilities. Thus they can be evaluated by the techniques of Vandermonde or Ceperley *et al.* Second, for the cases which interest us, the sum over β for fixed α has only a relatively small number of terms. For example, the kinetic energy has no more than $N_h z$ terms, where N_h is the number of holes (which is small when $1-n_f\ll 1$ and $n_f=N/L$ is the number of electrons per site) and z is the number of neighbors. Somewhat more time consuming is the off-diagonal part of $\sum_i \mathbf{s}_i\cdot\mathbf{s}_{i+1}$, which we compute for states of nonzero total magnetization. The number of terms can then approach L but are still manageable. Hence, for our purposes, off-diagonal operators present no special problems.

It is generally permissible in the Monte Carlo technique to decompose the summand as one wishes, one part going into determining the transition probabilities, the second to be averaged over. The most efficient method chooses the first part to have most of the variance, and the second to be as close to constant as possible. We are fortunate in this case that the requirement of ease of calculation seems to coincide with this prescription, since the kinetic energy converges reasonably well.

III. EFFECTIVE HAMILTONIAN

Our objective in this paper is to assess the appropriateness of the Gutzwiller wave function for a single-band Hubbard model:

$$H=-t\sum_{\langle i,j\rangle,\sigma} c_{i\sigma}^\dagger c_{j\sigma}+\text{H.c.}+U\sum_i n_{i\uparrow}n_{i\downarrow} , \tag{5}$$

in which U/t is large ($t>0$) but not infinite, and $\langle i,j\rangle$ are pairs of nearest-neighbor sites. In addition, our focus is on the nearly-half-filled band case $1-n_f\ll 1$. We then have, to order t/U, two contributions to the total energy. The first is just the hopping term, the energy associated with the motion of the relatively few holes. [We mean this term to be synonymous with "empty site." Our "holes" then propagate in the (lower) Hubbard band. This is distinct from its usage, in semiconductor physics, to mean an empty orbital in a nearly full Bloch band.] This energy vanishes when $n_f=1$ and is proportional to $-(1-n_f)t$ when $1-n_f$ is small. The second contribution is the energy of *virtual* hopping involving the creation and destruction of a nearest-neighbor (NN) hole–doubly-occupied-site pair. *Real* processes of this kind are negligible since they have an energy U. The virtual hopping takes place on pairs of singly occupied sites. The total is therefore proportional to n_f. The two terms become comparable when $U \sim t/(1-n_f)$, i.e., at larger U than one might naively expect. Following Castellani *et al.* and Hirsch,[19] we now transform the Hubbard Hamiltonian (5) to an effective Hamiltonian which describes these processes more precisely. We rewrite (5) as

$$\begin{aligned} H &= T_h + T_d + T_{\text{mix}} + V \ , \\ T_h &= -t \sum_{\langle i,j\rangle,\sigma} (1-n_{i,-\sigma})c_{i\sigma}^\dagger c_{j\sigma}(1-n_{j,-\sigma}) + \text{H.c.} \ , \\ T_d &= -t \sum_{\langle i,j\rangle,\sigma} n_{i,-\sigma}c_{i\sigma}^\dagger c_{j\sigma} n_{j,-\sigma} + \text{H.c.} \ , \\ T_{\text{mix}} &= -t \sum_{\langle i,j\rangle,\sigma} n_{i,-\sigma}c_{i\sigma}^\dagger c_{j\sigma}(1-n_{j,-\sigma}) + \text{H.c.} \\ &\quad - t \sum_{\langle i,j\rangle,\sigma} (1-n_{i,-\sigma})c_{i\sigma}^\dagger c_{j\sigma} n_{j,-\sigma} + \text{H.c.} \ , \\ V &= U \sum_i n_{i\uparrow} n_{i\downarrow} \ , \end{aligned} \tag{6}$$

with $n_{i,\sigma} = c_{i\sigma}^\dagger c_{i\sigma}$. T_h describes the transport of holes and T_d that of doubly occupied sites, i.e., T_h and T_d do not mix different Hubbard bands, only T_{mix} does so. We now apply an unitary transformation to (6),

$$H_{\text{eff}} = e^{+iS} H e^{-iS} = H + i[S,H] + \cdots \ , \tag{7}$$

and choose S so that T_{mix} vanishes in lowest order. We want to remove real mixing processes between different Hubbard bands. This yields the condition $i[S, T_h + T_d + V] = -T_{\text{mix}}$ or

$$S = \sum_{n,m} |n\rangle \frac{\langle n | T_{\text{mix}} | m \rangle}{i(\varepsilon_n - \varepsilon_m)} \langle m | \ , \tag{8}$$

where $|n\rangle, |m\rangle$ are eigenstates of $T_h + T_d + V$ with eigenvalues ε_m and ε_m. Except for one dimension, we do not exactly know ε_n and ε_m but, for the large-U limit, $\varepsilon_n - \varepsilon_m = \pm U + O(t)$. So we get

$$\begin{aligned} S = &-\frac{it}{U} \sum_{\langle i,j\rangle,\sigma} n_{i,-\sigma} c_{i,\sigma}^\dagger c_{j\sigma}(1-n_{j,-\sigma}) \\ &+ \frac{it}{U} \sum_{\langle i,j\rangle,\sigma} (1-n_{i,-\sigma}) c_{i\sigma}^\dagger c_{j\sigma} n_{j,-\sigma} \ . \end{aligned} \tag{9}$$

H_{eff} taken between states with no doubly occupied sites becomes

$$\begin{aligned} H_{\text{eff}} &= T_h + i[S, T_{\text{mix}}] \\ &= T_h + 2\tau \sum_{\langle i,j\rangle} (\mathbf{s}_i \cdot \mathbf{s}_j - \tfrac{1}{4}) \end{aligned} \tag{10}$$

for the case of spin $\frac{1}{2}$ ($N_f = 2$) and $\tau = 2t^2/U$. Note we work only to lowest order and drop all terms $O(t^3/U^2, (1-n_f)t^2/U, (1-n_f)^2 t)$. Notice that the expectation value $\langle \Psi_G | H_{\text{eff}} | \Psi_G \rangle$ is equal to $\langle \tilde{\Psi}_G | H | \tilde{\Psi}_G \rangle$ with $|\tilde{\Psi}_G\rangle = (1-iS)|\Psi_G\rangle$, neglecting terms of order t^2/U^2.

This means that we have a total number of doubly occupied sites,

$$D = \left\langle \tilde{\Psi}_G \left| \frac{1}{U} V \right| \tilde{\Psi}_G \right\rangle = -\frac{1}{2}\frac{1}{U} \langle \Psi_G | V_{\text{corr}} | \Psi_G \rangle \ , \tag{11}$$

if we write $H_{\text{eff}} = T_h + V_{\text{corr}}$.

This approach is different from that introduced by Kaplan *et al.*[15] to describe the case of U finite. They used a Gutzwiller wave function with a finite density of doubly occupied sites, but with an additional projection operator which retained only those configurations in which all doubly occupied and empty sites are on nearest-neighbor pairs. In this way they obtained a very good energy. Our approach gives an even better energy and has two additional advantages: (i) we keep the $U=\infty$ Gutzwiller wave function and put the changes into H_{eff}, which is easy to handle, and (ii) H_{eff} clearly separates two different physical processes, namely the propagation of holes (or doubly occupied sites) from the virtual processes which cause the Heisenberg spin-spin coupling. If we use the GAF as, for example, Brinkman and Rice[18] did, only the first term is included, but it is only these real propagation processes which can cause metallic conductivity. For an exactly half-filled band at large U, the first term must be zero and the system remains insulating. On the other hand, our method, as an expansion in t/U, is suitable only for the large-U limit, whereas Kaplan *et al.*,[15] with their approach, can discuss both limits.

In the case of higher degeneracy ($N_f > 2$), V_{corr} is no longer a Heisenberg antiferromagnetic spin-spin coupling, but

$$V_{\text{corr}} = \tau \sum_{\langle i,j\rangle} P_i P_j (T_{i,j}^{\text{mix}}/t)^2 P_i P_j \ , \tag{12}$$

where the P_i are projection operators which specify that the only matrix elements are between singly occupied sites. The interaction is again antiferromagnetic, but more in the sense of a quantum Potts model, rather than a Heisenberg model of higher spin.

A question that arises is the relation of this model to the case of the heavy-electron metals. These materials are described by a periodic Anderson model rather than a Hubbard model. It is plausible to conjecture that one can make a similar transformation of the Anderson Hamiltonian to a H_{eff} which again splits into kinetic-energy (or propagation) terms and spin-spin–coupling terms. Indeed, Hirsch[19(b)] has proposed that the form of H_{eff} for the Hubbard and Anderson models is the same. He assumed that the f-level energy E_f lies well below the Fermi energy, but the various approximate treatments[10–14] and the Monte Carlo calculations of Shiba[17] show that E_f is renormalized to the Fermi energy and therefore the expansion proposed by Hirsch breaks down. Indeed, the essence of the heavy electron problem (see, for example, Rice and Ueda[10]) is that the hybridization or kinetic-energy terms are essentially nonanalytic in $1-n_f$, in contrast to the Hubbard model, where an analytic expansion is expected. Nonetheless, it is plausible that a qualitatively similar form of H_{eff} can be found in which the hybridization terms evaluated exactly by Shiba[17] are supplemented by spin-spin terms which can also be evaluated exactly by Monte Carlo techniques.

IV. GROUND-STATE RESULTS

In this section we discuss the results of the Monte Carlo calculations for the ground state in one dimension, as a function of the band filling, magnetization, and degeneracy, N_f, parameters. In Sec. IV A we concentrate on the NN spin correlations, while in Sec. IV B we focus on the kinetic energy, in Sec. IV C we discuss the spatial correlations between holes (empty sites) in the Hubbard band. In Sec. IV D we present results for the momentum distribution function $n(k)$ and in Sec. IV E we will consider the implications of the results taken together.

A. Nearest-neighbor correlations

For spin $\frac{1}{2}$ and a half-filled band, Horsch and Kaplan[16(a)] calculated the NN spin correlation $q_1=\langle s_i^z s_{i+1}^z\rangle$ for chains up to 98 sites. Their extrapolated result for $L\to\infty$ is $q_1=-0.1474\pm0.0007$.

The exact (Bethe-ansatz solution) result for the antiferromagnetic Heisenberg chain (AFH) is[22]

$$q_1^{\mathrm{AFH}}=-\tfrac{1}{3}(\ln 2-\tfrac{1}{4})=-0.147\,7157\ldots \quad (13)$$

This value is about 0.2% above, but within, the error bars of the result of Kaplan *et al.* This opens the question of whether the Gutzwiller wave function for the Hubbard model in one dimension and for the half-filled band is identical to the exact antiferromagnetic ground state.

To answer this question we performed calculations, with the Vandermonde method, for chains with up to 6000 sites, with 10^4–10^5 MC steps per site. The extrapolated result of a fit of the form $q_1(L)=q_1(\infty)+\Delta q/L^2$ is (see Fig. 1)

$$q_1(\infty)=-0.147\,39\pm0.000\,02 \ . \quad (14)$$

The exact AFH value (13) differs by several standard deviations from our result (14), so that we conclude that the half-filled-band Gutzwiller wave function is *not* identical to the AFH ground state.

We have also investigated the change in the spin correlation in the presence of a uniform magnetization $m=2\langle s_i^z\rangle$. In this case $\langle s_i^z s_{i+1}^z\rangle\neq\langle s_i^x s_{i+1}^x\rangle$ $(=\langle s_i^y s_{i+1}^y\rangle)$, so that one must calculate both expectation values. As we discussed above, the calculation of $\langle s_i^x s_{i+1}^x\rangle$ is more complicated as it involves off-diagonal operators (e.g., $s_i^- s_{i+1}^+$). Nonetheless, we found that runs of 2×10^4 MC steps per site for chains up to $L=210$ were possible. We made a fit to a quadratic dependence for the deviation in $\langle \mathbf{s}_i\cdot\mathbf{s}_{i+1}\rangle$, and then if we use the effective Hamiltonian, H_{eff}, it is straightforward to calculate the change in energy. The uniform susceptibility χ is then easily obtained by expanding the energy per particle

$$\varepsilon(m)=\varepsilon(0)+g^2\mu^2m^2/2\chi \ , \quad (15)$$

and we find, for the half-filled band,

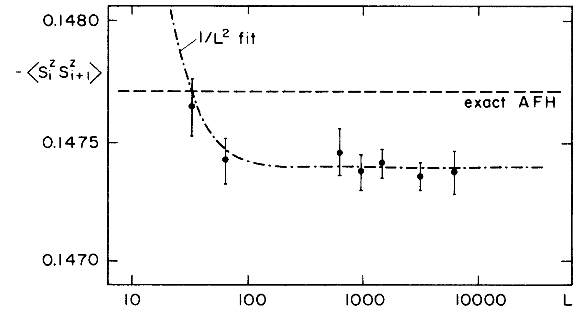

FIG. 1. Nearest-neighbor spin correlations. Shown are some of the 18 data points that were used to obtain the fit $\langle s_i^z s_{i+1}^z\rangle=q_1(\infty)+\Delta q_1/L^2$. L ranges from 18 to 6010. Total number of Monte Carlo steps is 6×10^7 for all large samples. Also shown is the value for the exact ground state of the antiferromagnetic Heisenberg chain (AFH).

$$\chi_{\mathrm{Gutz}}=0.058\pm0.008\frac{g^2\mu^2}{\tau} \ . \quad (16)$$

This value of χ is also very close to the exact value of the AFH chain:[23]

$$\chi_{\mathrm{AFH}}=\frac{1}{2\pi^2}\frac{g^2\mu^2}{\tau}=0.0506\frac{g^2\mu^2}{\tau} \ . \quad (17)$$

Note that χ_{Gutz} is slightly higher than χ_{AFH}. This means that for higher values of the magnetization m, the difference in energy between the Gutzwiller wave function and the AFH chain becomes smaller. This is to be expected since in the limit $m=1$ they are identical.

Now we turn to higher values of the degeneracy N_f. The effective Hamiltonian is given in (12). Figure 2 shows the result for $\langle V_{\mathrm{corr}}\rangle$. For the Gutzwiller state $\langle V_{\mathrm{corr}}\rangle$ approaches -2τ per site asymptotically for large N_f. This is remarkable, since -2τ per site is an absolute lower bound. To see this, we note that the eigenvalues of V_{corr} for the two-site problem are 0 and -2τ for all N_f.

It is amusing to make a comparison between the

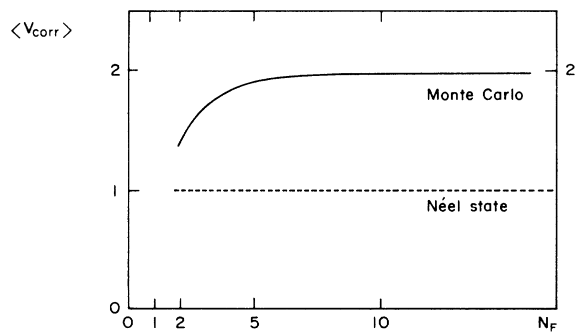

FIG. 2. Expectation value of the correlation energy $\langle V_{\mathrm{corr}}\rangle$ [defined in (12)], in units of $-2t^2/U$ as a function of degeneracy N_f, for the Gutzwiller wave function (Monte Carlo) and the Néel state. Note that the MC result approaches $-4t^2/U$ asymptotically for large N_f. L ranges from 60 to 240 (for large N_f) and 2000 MC steps per site were used.

Gutzwiller and Néel states, which is the ground state for an antiferromagnetic Heisenberg $\mathbf{s}_i \cdot \mathbf{s}_j$ interaction in the classical limit $S \to \infty$. (S is similar to the degeneracy N_f.) However, the ground state for the effective Hamiltonian (12) does not approach the Néel state, which has $\langle V_{\text{corr}} \rangle = -\tau$ for all N_f. Thus, for large N_f the Gutzwiller wave function yields about twice the correlation energy of the Néel state. Note that the conclusion that the Gutzwiller state is energetically favored over the Néel state is a consequence of the form of the coupling (12). Finally, in Fig. 3 we plot the results of the nn spin correlation as a function of N_f.

These results change only slightly when we introduce a small number of holes, $1-n_f$. The decrease in $\langle V_{\text{corr}} \rangle$ and $\langle \mathbf{s}_i \cdot \mathbf{s}_{i+1} \rangle$ is found to be only $\sim (1-n_f)$, as expected.

B. Kinetic energy for a less than half-filled band

In this subsection we will show that the Gutzwiller wave function when we introduce a few holes $(1-n_f > 0)$ yields a good kinetic energy with respect to the exact values, and that the GAF is a good approximation for the kinetic energy. This is important since the Gutzwiller wave function is a coherent wave function with a Fermi surface enclosing n_f states per site. The exact ground state of the infinite-U Hubbard model (see Klein and Seitz[24] and Brinkman and Rice[18] for a description), on the other hand, is not coherent in the sense that it has a finite mobility. Further, the one-particle Green's function for a single hole introduced into an infinite-U Hubbard chain does not have a quasiparticle pole.[18]

Figure 4 shows the kinetic energy per hole in the limit of small hole density $1-n_f$. The exact value of the Hubbard model in one dimension for a state with a given spin configuration is $-2t$.[24]

The GAF for the ground-state kinetic energy per site is (see Ref. 10) (in one dimension)

$$\varepsilon_{\text{Gutz}} = \sum_{\sigma=1}^{N_f} \frac{1-n_f}{1-n_\sigma} \langle \varepsilon_\sigma \rangle = -\frac{(1-n_f)N_f}{1-n_f/N_f} \frac{2t}{\pi} \sin\left[\frac{n_f \pi}{N_f}\right] . \tag{18}$$

Formula (18) yields a value below the exact value, $-2t$

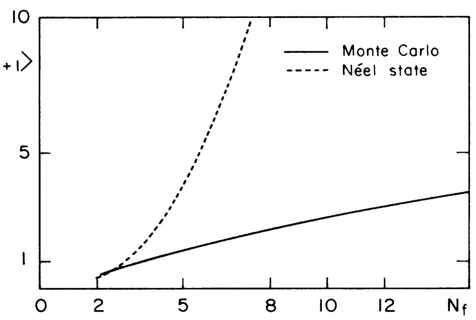

FIG. 3. Nearest-neighbor spin correlation $\langle s_i^z s_{i+1}^z \rangle$ as a function of degeneracy N_f. The results for the Gutzwiller wave function (Monte Carlo) and for the Néel state are shown. L varies from 60 (for small N_f) to 280 (for large N_f). 2000 MC steps per site were used.

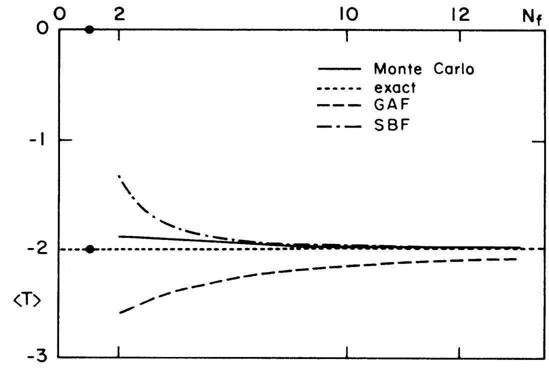

FIG. 4. Expectation value of the kinetic energy per hole as a function of degeneracy N_f. The results are shown for the Gutzwiller wave function (Monte Carlo), the Gutzwiller approximate formula (GAF), the slave-boson formula (SBF), and for the exact ground state. Note that the special value $N_f = 1$ lies off the smooth curve obtained for $N_f \geq 2$ and that in this case the SBF yields zero instead of the exact value $-2t$, obtained in the GAF. $L = 240$ and 10^4 MC steps per lattice site were employed.

per hole, because in one dimension the density of states has a quadratic divergence at the band edges and $\langle \varepsilon_0 \rangle$ gets pushed below the median. This changes in higher dimensions and we expect that the GAF will improve in accuracy in higher dimensions.

Other authors have proposed to use formula (18) without the factor $1/(1-n_\sigma)$. Such a formula follows from the simplest slave-boson approach and we will call this the slave-boson formula (SBF). The corresponding values are also shown in Fig. 4. We see that in one dimension one cannot decide between these two possibilities from the ground-state expectation value of the kinetic energy alone. Especially in the large-N_f limit both converge to $-2t(1-n_f)$, as does the MC result. For large N_f the SBF seems to be a better approximation to the MC result, although for $N_f = 1$ it goes to 0, whereas (18) yields the correct value, $-2t$, per hole. As we noted above, there are grounds to believe that the GAF is better in higher dimensions.

The ground-state expectation values of the kinetic energy for a general value of the band filling, $0 \leq n_f \leq 1$ and $N_f = 2$, are shown in Fig. 5. We see that the Gutzwiller wave function is in good agreement with the exact ground state in the mixed-valence regime $n_f \approx \frac{1}{2}$ and that both the Monte Carlo calculations and the GAF, (18), yield a good overall agreement, in contrast to the SBF, which gives an overly small kinetic ground-state energy in this regime.

Next, we consider the change of the kinetic energy with a finite magnetization m for the case $N_f = 2$. If we write $\varepsilon_{\text{Gutz}}(m^2) = \varepsilon_0(1 - am^2)$, then we have for the GAF a value

$$a = (1/\rho - 1) , \tag{19}$$

while for the SBF we get

$$a = 1/\rho , \tag{20}$$

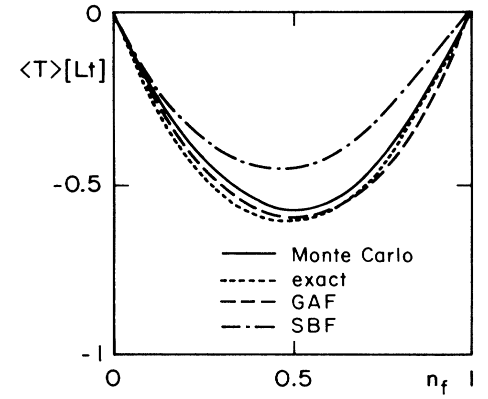

FIG. 5. Kinetic energy per site for $N_f=2$ as a function of the band filling n_f. The results are shown for the Gutzwiller wave function (Monte Carlo), the Gutzwiller approximate formula (GAF), the slave-boson formula (SBF), and the exact ground state (Ref. 25). $L=100$ and 10^4 MC steps per site were used.

with $\rho=2N(0)|\varepsilon_0|$; $N(\varepsilon)$ is the density of states for both spins, and $\varepsilon_0=\int_{-\infty}^{0} N(\varepsilon)\varepsilon\, d\varepsilon$. (The energy zero is always taken as the Fermi energy when $n_f=1$ and $m=0$.) In three dimensions ρ is slightly greater than 1 [Ref. 1(d)] so that (19) is negative, which leads to a magnetic instability.[10]

In one dimension and for nearest-neighbor hopping, $\rho=8/\pi^2$ and $\rho^{-1}\simeq 1.23$, so that a is reduced by a factor of 5 relative to (20). To test these formulas we have performed MC calculations with a finite magnetization with the result $a=0\pm0.05$. So the MC result is far below both values, at least a factor of 5 lower than (19) and a factor of 25 lower than (20). Clearly, the SBF is a very bad approximation for the spin susceptibility of the Gutzwiller wave function.

The fact that a is so small, probably zero, is a consequence of the high spin degeneracy of the exact ground state.[24] Indeed, for the exact solution, $a=0$ for $U=\infty$ (Ref. 25) since the hole moves freely in any given spin configuration in one dimension. In higher dimensions this would not be the case.

C. Hole-hole correlations

For a noninteracting gas of electrons, empty sites, or holes as defined in Sec. III, cannot be regarded as particles, since neither their total number is conserved nor do they obey Fermi statistics, as they can be created either with an odd or even number of fermion operators. Their spatial correlation function is induced by that of the electrons and is given ($N_f=2$) in the half-filled case by

$$\langle\Psi_0|h_r h_{r'}|\Psi_0\rangle=n_h^2[g_{\sigma,\sigma}(r-r',k_F^e)]^2\ ,$$

where $h_r=1$ or 0, depending on whether there is a hole or not on site r, n_h is the average density of holes ($n_h=\frac{1}{4}$), and $g_{\sigma,\sigma}(r,k_F^e)$ is the parallel spin-correlation function of the noninteracting electron gas, with Fermi wave vector k_F^e. In one dimension $g_{\sigma,\sigma}(r,k_F^e)$ is given by

$$g_{\sigma,\sigma}(r,k_F^e)=1-\left[\frac{\sin(k_F^e r)}{(Lk_F^e/\pi)\sin(\pi r/L)}\right]^2 , \tag{21}$$

where L is the lattice size. From (21) it follows that the correlation length for the empty sites is about $1/k_F^e$, i.e., about a lattice constant.

This situation now changes dramatically when we consider an almost-localized liquid. In one dimension, holes on the infinite-U Hubbard model can be regarded as a noninteracting gas of spinless fermions.[24] For the case of N_h holes in L sites, the exact eigenstates are characterized by N_h k vectors, chosen out of L possible values. Each of these states has a large spin degeneracy of $N_f^{L-N_h}$.[24] The hole-hole correlation function is given by

$$g_{h,h}^e(r)=g_{\sigma,\sigma}(r,k_F^h)\ , \tag{22}$$

where k_F^h is the Fermi wave vector of the hole Fermi sea. Note that (22) is independent of N_f, magnetization, and spin configuration. Around each empty site a "Fermi hole" exists, a region with reduced probability of finding another hole. The radius of this Fermi hole is of order $1/k_F^h$, which is about the mean distance between two empty sites. This correlation length may be quite large for a small hole concentration.

Since the Gutzwiller wave function is not the exact ground state of the kinetic energy, we do not expect to find (22) exactly as the correlation function. We have calculated the hole-hole correlation function for the Gutzwiller wave function and the results for different densities are shown in Fig. 6.

We see that the overall shape of the correlation function for the Gutzwiller function $g_{h,h}^{\rm Gutz}$ and that for the free hole liquid $g_{h,h}^e$ are in good agreement. We now discuss several distinct features.

In r space we notice that the radius of the "Fermi hole"

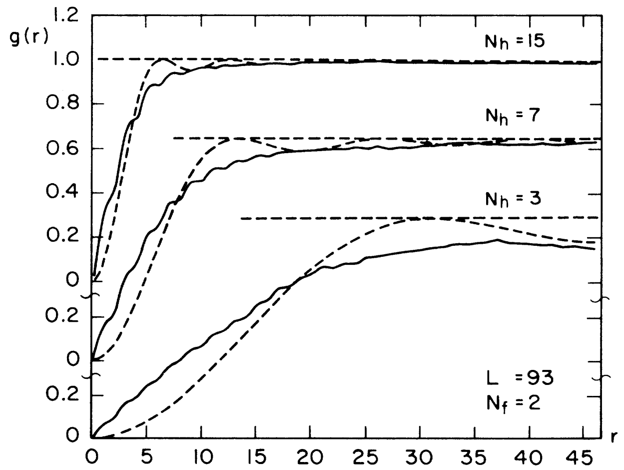

FIG. 6. Hole-hole correlation function $g_{h,h}(r)$ in real space for three samples. The degeneracy $N_f=2$, the lattice size $L=93$, and the number holes is $N_h=3,7,15$. the results are shown for the Gutzwiller wave function (solid line) and $g_{h,h}^e(r)$ [see Eq. (22)] (dashed line). The dashed line at $g(r)=1$ is a guide to the eye. About 10^5 MC steps per site were used.

follows that of the free-hole liquid (about the mean distance between two holes), but the characteristic oscillations with wavelength $2k_F^h$ are suppressed. This is to be expected since these oscillations derive from a sharp hole Fermi surface, which is not present in the Gutzwiller state. This one sees clearly inspecting the hole-hole correlation in k space. The Fourier-transformed hole-hole correlation for the same samples ($N_f=2$, $L=93$, number of holes is 3, 7, and 15) is shown in Fig. 7. This function for the free-hole liquid is

$$g_{h,h}^{e}(k)=\begin{cases}\left[\frac{1}{L}\right]^{1/2}\frac{\pi}{k_F^h}\left[1-\frac{k}{2k_F^h}\right], & k<2k_F^h\\ 0, \quad k>2k_F^h .\end{cases} \tag{23}$$

The sharp cutoff for $k>2k_F^h$ is due to the sharp Fermi surface, while $g_{h,h}^{\rm Gutz}(k)$ goes smoothly towards zero. An interesting feature in $g_{h,h}^{\rm Gutz}(k)$ is a kink at exactly $2k_F^e$ (k_F^e is the Fermi wave vector of the underlying electron Fermi sea), together with a rise for $k>2k_F^e$. This illustrates that the Gutzwiller wave function has a discontinuity in k space at k_F^e, as required for a Fermi liquid to satisfy Luttinger's theorem (also see Sec. IV D).

This last feature is also seen in $g_{h,h}^{\rm Gutz}(r)$, in the short-range oscillations. Note that there are additional small bumps, especially for $N_h=3$, due to limited numerical accuracy.

Another intriguing feature of the hole-hole correlation functions is the systematic enhancement of $g_{h,h}^{\rm Gutz}(r)$ for small r with respect to $g_{h,h}^{e}(r)$. One possible explanation might be a built-in effective short-range attraction between the holes in the Gutzwiller wave function. The origin of this phenomenon is at present not understood.

In conclusion, we have found a remarkable correspondence between the hole-hole correlation function of the Gutzwiller state and a free-hole Fermi liquid.

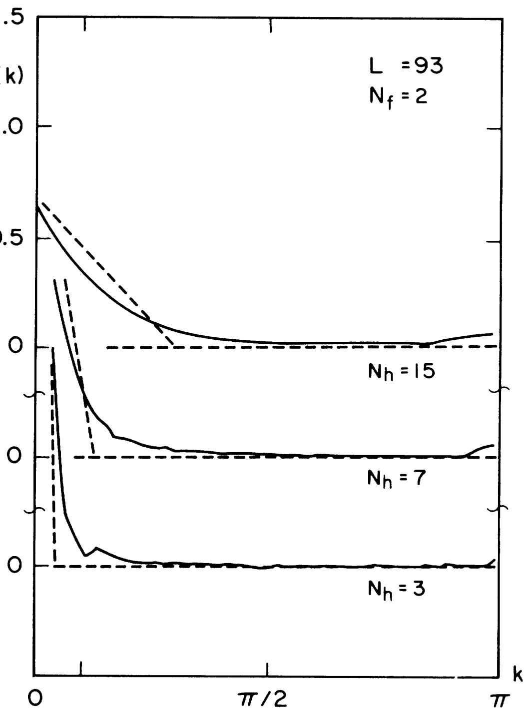

FIG. 7. Hole-hole correlation function $g_{h,h}(k)$ in k space for three different samples. The degeneracy $N_f=2$, $L=93$, $N_h=3,7,15$. The results are shown for the Gutzwiller wave function (solid line) and $g_{h,h}^{e}(k)$ [see Eq. (23)] (dashed line). About 10^5 MC steps per site were used.

D. Momentum distribution functions

We have calculated $n(k)$ for two values of n_f, $\frac{90}{93}$ and $\frac{86}{93}$. For $n(k)$ we used $n(k)=c_{k,\sigma}^{\dagger}c_{k,\sigma}$, valid for $U=\infty$. For finite but large U we would have to use $\tilde{n}(k)=n(k)+i[S,n(k)]+\cdots$ [see (7)]. The results are shown in Fig. 8 together with $n(k)$ calculated using the GAF. The Fermi surface is reproduced exactly in accordance with Luttinger's theorem. Within the Fermi sea $n(k)\equiv 1-n_f/2$, as one can also show analytically.[2] The depletion of $n(k)$ for $k>k_F$ near the Fermi surface is unexpected and results in a jump at the Fermi surface nearly twice as large as that given by the GAF of $(1-n_f)/(1-n_f/2)$. This extra depletion has implications for the use of GAF for excited states and we will return to this point later in Sec. V.

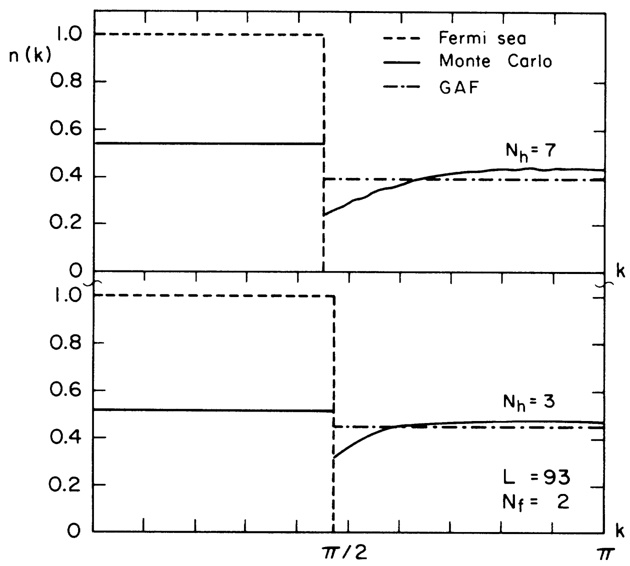

FIG. 8. Distribution function in momentum space $n(k)$. The dashed line is the noninteracting Fermi sea. Results are shown for the Gutzwiller wave function (Monte Carlo) and the Gutzwiller approximation (GAF). About 10^5 MC steps per site were used.

E. Total energy

In this subsection we consider the implications when we combine the results for the spin correlations and the kinetic energy of the holes. In the limit that U is large but finite ($U/t \gg 1$), and the density of holes is small ($0 < 1-n_f \ll 1$), both terms in the effective Hamiltonian will contribute. In this case the energy of $|\Psi_G\rangle$ is simply the sum of the two terms,

$$\langle \Psi_G | H_{\rm eff} | \Psi_G \rangle = -\alpha(1-n_f)2t - \beta\frac{4t^2}{U} + O\left[(1-n_f)\frac{t^2}{U}\right] . \quad (24)$$

The two coefficients α and β are very close to the best possible values. The value of α is discussed in Sec. IV B and illustrated in Fig. 4. The deviation between the maximum possible value (i.e., $\alpha=1$) and the values shown in Fig. 4 for $N_f=2$ is $\simeq 6\%$. The coefficient β is determined by the value of $\langle \mathbf{s}_i \cdot \mathbf{s}_{i+1} \rangle$ and, as discussed in Sec. IV A, this deviates by only 0.2% from the maximum possible given by the solution of the Heisenberg chain. Thus it is clear, at least in this case, that the almost-localized Gutzwiller state is an excellent compromise choice which comes close to maximizing both contributions. Also, neither T_h nor T_d in $H_{\rm eff}$ [Eq. (6)], when operating on $|\Psi_G\rangle$, generate empty or doubly sites. Therefore, $|\Psi_G\rangle$ remains the lowest-energy state of $H_{\rm eff}$, even if one considers the more general class of Gutzwiller wave functions in which d is allowed to be finite.

The interest in this limit lies in its relation to the heavy-electron systems. Such systems are described by the periodic Anderson model. In the case of an asymmetric Anderson model, a small number of electrons are promoted out of the otherwise integrally occupied f level which then can coherently hybridize with the conduction band. If we then consider the f-electron band itself, it can be thought of as an almost-half-filled Hubbard model, but the distribution of occupied f Bloch states in $\mathbf{k}$ space is determined now by the hybridization term and is therefore quite different than that in the Hubbard model. Shiba's MC calculations[17] on the Anderson model also show strong short-range spin-spin correlations. However, in his calculations only the energy of the band hybridization is included, analogous to including only the first term in Eq. (24). It is therefore plausible that a further gain in energy in addition to the terms that Shiba calculated should come from the spin-spin correlation through the Ruderman-Kittel-Kasuya-Yosida (RKKY) coupling analogous to the second term of Eq. (24). Indeed, Hirsch[19(b)] and recently Cyrot[19(c)] have proposed effective Hamiltonians for the periodic Anderson model which have a form similar to $H_{\rm eff}$ defined in Eq. (10). However, in the periodic Anderson model it is essential to retain the hybridization form of the effective Hamiltonian to obtain a finite value of $1-n_f > 0$ (see Ref. 1) and this, in turn, changes the form of the spin correlations. Therefore there remain, it seems to us, some important differences between the two models which should be reflected in the effective Hamiltonian. However, it is clear that the coherent hybridization term is not simply a one-band hopping term and Hirsch's treatment does not properly account for the renormalization of the effective f level to the Fermi energy.

V. EXCITED STATES

In this section we look at the properties of the excited-state Gutzwiller wave functions. These functions have the form $|\Psi_G^{\rm ex}\rangle = P|\Psi_{\rm ex}\rangle$, where P is the same projection operator as before and $|\Psi_{\rm ex}\rangle$ is an excited-state wave function of the noninteracting system. We are interested in the properties of these states because they should be representative of properties of the system at temperatures higher than the renormalized Fermi temperature. This temperature is $\sim(1-n_f)t$ and therefore is much lower than U or t. We should point out that the statistical mechanics of these excited states is nontrivial because of the overcompleteness of this set of Gutzwiller states.[26]

For example, in the subspace of zero total z component of spin, there are $\{L!/[(L/2)!]^2\}^2$ possible choices of these functions in a half-filled band of L sites. Each choice corresponds to a momentum distribution of the noninteracting function. It is easy to see in the site representation, however, that the dimension of the space in question is actually $L![(L/2)!]^2$, a far smaller number. Here we deal only with the properties of individual states and avoid the issue of entropy. It is good to bear in mind, however, that the states we discuss are *not* mutually orthogonal.

To begin with we examine highly excited states characteristic of temperature $T > (1-n_f)t$. These are constructed by taking the ground-state k distribution

$$\{-k_F, -k_F+2\pi/L, \ldots, 0, \ldots, k_F\} ,$$

and expanding it by a constant factor α (see Fig. 9). That is, when $k_i > 0$, then

$$k_i < \frac{2\pi}{L} I\left[\alpha\frac{L}{2\pi}k_i\right] ,$$

where $I(x)$ denotes the maximum integer less than or equal to x. If $k_i < 0$, then the new k are determined by the requirement that the new distribution is symmetric about 0. The new $\{k_i\}$ then respect the periodic boundary conditions. If α is itself an integer, then this just corresponds to a constant multiplication of the interval between the $\{k_i\}$, and the Vandermonde method may be used for to find expectation values. Otherwise, the method of Ceperley *et al.* is used. If $\alpha > 2$, then the k values may lie in higher Brillouin zones and care must be taken in the choice of L so that no $\{k_i\}$ are related by a Bragg reflection. Results for choices of α are given in Table I for the spin-correlation functions and the kinetic energy for systems with a single hole.

The first row of the table shows that the spin correlations in the wave function are crucially dependent on the k distribution. As the k distribution becomes more uniformly distributed over the zone, the NN correlations change from antiferromagnetic to ferromagnetic. We can understand this in the following way. In the Gutzwiller ground state, the average *magnitude* of the wavevectors is $\pi/4$. A wave for a given spin thus will tend to have the maxima of its associated probability separated by two sites. A similar wave for the other spin will have the same property, but the projection operator will enforce the

TABLE I. Results for various excited states characterized by an expansion factor α, as described in the text. Values for $\alpha=1,2,4$ are for systems with 78 electrons, 79 sites, and 2.5×10^4 MC steps per site. For $\alpha=\frac{7}{6}$, $\frac{4}{3}$, $\frac{3}{2}$, $\frac{5}{3}$, and $\frac{11}{6}$ the corresponding parameters are 30, 31, and 5×10^4. Kinetic energies are given in units of t, per hole, for the results of the MC calculations ($\varepsilon_{\rm MC}$) and the Gutzwiller approximate formula ($\varepsilon_{\rm GAF}$).

α	1	$\frac{7}{6}$	$\frac{4}{3}$	$\frac{3}{2}$	$\frac{5}{3}$	$\frac{11}{6}$	2	4
$\langle \mathbf{s}_i\cdot\mathbf{s}_{i+1}\rangle$	-0.439 ± 2	-0.379 ± 6	-0.265 ± 7	-0.142 ± 9	-0.086 ± 21	-0.006 ± 46	0.165 ± 36	0.048 ± 40
$\langle \mathbf{s}_i\cdot\mathbf{s}_{i+2}\rangle$	0.162 ± 3	0.106 ± 7	0.020 ± 9	-0.038 ± 11	-0.027 ± 28	0.024 ± 37	0.083 ± 45	0.000 ± 13
$\varepsilon_{\rm MC}$	-1.89 ± 1	-1.65 ± 6	-1.38 ± 10	-1.29 ± 6	-0.99 ± 12	-0.96 ± 9	-1.22 ± 27	0.85 ± 31
$\varepsilon_{\rm GAF}$	-2.51	-2.46	-2.00	-1.52	-1.13	-0.074	-0.0005	0.0005

condition that the maximum of one wave will coincide with the minimum of the other. The wave functions for different spins thus mesh in such a way as to give antiferromagnetic correlations. Alternatively, one may say that the exchange hole has just the right size to cooperate with the smaller projection hole to give a high probability of opposite spins on neighboring sites. When α equals 2, on the other hand, the probability maxima for like spins are only separated by one site and we even get ferromagnetic NN correlations. Intermediate values of α interpolate between these extremes. $\alpha=4$ is similar to $\alpha=2$, by the same argument, since in this case the wave vectors are also roughly uniformly distributed in the first zone. The application of the same reasoning to the next-nearest-neighbor (NNN) correlation indicates that, as α goes from 1 to 2, the NNN correlation should change from ferromagnetic to antiferromagnetic and finally back to ferromagnetic. This expectation is borne out by the first and second rows of the table.

We now turn to the kinetic energy. The first and most basic fact is that the ground state ($\alpha=1$) does in fact have a lower kinetic energy than all other Gutzwiller states, as seen in the third row of the table. In fact, as the momentum distribution expands, the kinetic energy increases quite rapidly at first, then more slowly, leveling off when the uniform distribution is approached. Second, the Gutzwiller ground state has a kinetic energy within 10% of that of the (highly degenerate, $U=\infty$) exact ground state, $-2t$ in our units. The latter has the hole uniformly distributed in a background whose spin configuration is arbitrary. What is interesting about the development of the kinetic energy as α increases to 2 is that it remains negative, which is below the average energy of the exact eigenstates at $U=\infty$. This is an indication that most of our overcomplete set is concentrated in the low-energy

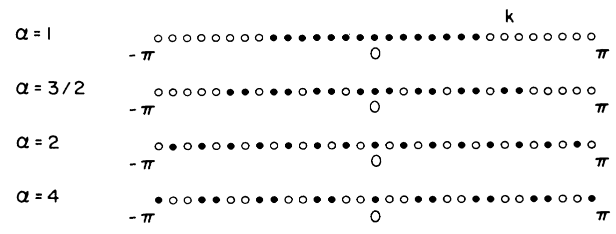

FIG. 9. Distribution of k states for some excited states calculated. The solid circles represent the occupied states. $\alpha=1$ corresponds to the ground state.

part of the state space, qualitatively confirming the form of the ansatz used by Seiler *et al.*[26] in their phenomenological description of the entropy of the states.

The Gutzwiller approximation for the kinetic energy of the excited states gives too low a value for states near the ground state. This comes from the fact that the denominator in (18) overestimates the blocking effect of like spins in one dimension, where, unlike two and three dimensions, the electrons are effectively spinless. This problem should not survive in higher dimensions. A second defect of the Gutzwiller approximation for the expectation value of the hopping term in $|\Psi_G^{\rm ex}\rangle$ is that it merely scales as the free kinetic energy. However, it is now evident from the foregoing discussion that when the projection operator is present finer details of the momentum distribution may become important. This is illustrated by the difference in kinetic energy between the $\alpha=2$ and 4 states. When $\alpha=2$, the $\{k_i\}$ are

$$\frac{2\pi}{L}\{\ldots,-4,-2,0,2,4,\ldots\}\ ,$$

whereas for $\alpha=4$, the distribution is

$$\frac{2\pi}{L}\{\ldots,-8,-7,-4,-3,0,3,4,7,8,\ldots\}\ .$$

Both are more or less uniform, but the correlations in k space are quite different. It is therefore not so surprising that the kinetic energies for $\alpha=2,4$ are so different, the kinetic energy being, after all, a short-range (off-diagonal) correlation in real space.

It is also of interest to examine the low-lying excited states. Since the energy difference between these states and the ground state is small, the use of the Vandermonde method is indispensable. The following one- and two-particle states are accessible to this method,

$$\begin{aligned}|\Psi_{\rm ex}^1\rangle &= c_{k'\uparrow}^\dagger c_{k_F\uparrow}|\Psi_0\rangle\ ,\\ |\Psi_{\rm ex}^2\rangle &= c_{k'\uparrow}^\dagger c_{k'\downarrow}^\dagger c_{k_F\uparrow}c_{k_F\downarrow}|\Psi_0\rangle\ ,\end{aligned}\tag{25}$$

with $k'=k_F+\Delta k$, $\Delta k=2\pi/L$. In the Appendix we show that the determinants we require are of the Vandermonde form multiplied by the symmetric factors $\sum_m z_m$ and $\sum_m z_m'$. The results of these calculations are shown in Tables II and III. Even with the use of the Vandermonde method the accuracy is limited since we have to subtract two large numbers.

We first turn to the results for the kinetic energy, shown in Table II. In the first three rows results are presented for one hole in chains of increasing length L. From Landau theory and the fact that the effective mass is proportional to $(1-n_f)^{-1}$, we expect that the total-energy difference $\Delta\varepsilon=\Delta\varepsilon_{\rm ex}-\varepsilon_g$ should scale with $(1-n_f)\Delta k$. The sixth column of Table II shows that this occurs within the numerical accuracy. The seventh column shows the values obtained by the GAF. We see that the GAF systematically overestimates $\Delta\varepsilon$, i.e., it underestimates m. The eighth column shows the values for the SBF. As for the total kinetic energy, the MC result lies in between the GAF and SBF (see Sec. IV B).

In Sec. IV D we presented the results for the momentum distribution function. If the self-energy is k independent and a function only of the energy variable, then the discontinuity at the Fermi surface is simply equal to m/m^*. The fact that we find that the effective mass is substantially larger than that given by the GAF, while at the same time the discontinuity in the momentum distribution is nearly twice as large than that given by the GAF, implies that the momentum dependence of the self-energy is substantial.

The last row of Table II shows the results of calculation for $N_h=7$, $L=93$, i.e., a large hole density $(1-n_f)$. In this case the ratio $\Delta\varepsilon\, nc/[(1-n_f)\Delta k]$ is much larger than the previous case, where $1-n_f$ was smaller. This implies that m/m^* has a substantial correction to the linear behavior in $1-n_f$ predicted by the GAF and SBF.

Lastly, we discuss the change in the spin-correlation function. We are interested in the contributions $\sim(1-n_f)\Delta k$ and $\sim(\Delta k)^2$. To distinguish these terms we have calculated Δq_1 first for the same conditions as for the kinetic energy $(1-n_f>0,\ \Delta k>0)$ and second for the half-filled case $(1-n_f=0,\ \Delta k>0)$ (see Table III). This is necessary since for the case of one hole $1-n_f\sim\Delta k$ and, therefore, we need both calculations to distinguish the two contributions. For $L=93$ the numerical accuracy is again too limited for any definite conclusion.

From the results for the half-filled case we deduce that Δq_1 is dominated by the term $\sim(\Delta k)^2$, and from comparison with the results for the cases with one hole we see that the contribution $\sim(1-n_f)\Delta k$ to Δq_1 is at most 10%. This now has a very interesting consequence, namely that the contribution of the spin-correlation energy to the linear specific heat is very small. This follows directly out of the Landau theory for Fermi liquids since $\Delta q_1\sim(\Delta k)^2$ and not of order Δk. We have seen before (Sec. IV E) that the spin susceptibility, on the other hand, is dominated by the spin-correlation energy. Then we have for the Wilson ratio

$$\chi/c_v\sim(t^2/U)^{-1}/[(1-n_f)t]^{-1}\sim U(1-n_f)/t\sim 1$$

in the regime in which we are working, i.e., where both terms of $H_{\rm eff}=T_h+V_{\rm corr}$ yield a comparable contribution to the ground-state energy (see Sec. IV E). This is clearly in accordance with experiments for heavy-electron metals.[1]

The main conclusion we wish to draw from this section is that the Gutzwiller ground state is distinguished from the excited states *both* by having a very low kinetic energy *and* very strong antiferromagnetic correlations. We have seen that the "filled Fermi sea," in conjunction with the projection operator, is ideal for producing these two effects simultaneously.

VI. CONCLUSIONS

In this work we examined various properties of Gutzwiller wave functions using a Monte Carlo technique to numerically evaluate the expectation values. Our calculations were restricted to one dimension only to achieve better numerical accuracy, but our interest is really in three dimensions, where a Fermi-liquid state is possible and the Gutzwiller wave function can be expected to be a good approximation.

Two clear results emerge from this work. First, the approximate formulas that Gutzwiller derived many years ago give a good value of the kinetic energy and the magnetic susceptibility. The agreement between our results is not perfect, however, and our MC results for the kinetic energy in one dimension taken at face value lie in between the GAF and SBF, the latter being the simplest slave-boson formula. However, there are reasons to believe that in higher dimensions the GAF will be a better approximation than the SBF. If we look at the spin dependence of the kinetic energy, then the agreement with the GAF is decidedly better than the SBF.

TABLE II. Results for excited states where an up and a down electron $(N_f=2)$ have been excited by $\Delta k=2\pi/L$ from the Fermi surface. Here, L and N_h are the number of sites and holes, and $1-n_f=N_h/L$ is the density of holes. $\Delta\varepsilon_{\rm MC}$, $\Delta\varepsilon_{\rm GAF}$, and $\Delta\varepsilon_{\rm SBF}$ are the differences of the expectation value of the kinetic energy relative to the ground state in units of t, for the results of the MC calculations, the Gutzwiller approximation formula (GAF), and the slave-boson formula (SBF), respectively. These energies divided by $(1-n_f)\Delta k$ yield the effective masses (last three columns). Note that the density of holes, $1-n_f$, for the fourth row is about twice as large as for the other samples. The corresponding effective mass (sixth column) is anomalously high.

L	N_h	$1-n_f$	Δk	$\Delta\varepsilon_{\rm MC}$	$\frac{\Delta\varepsilon_{\rm MC}}{(1-n_f)\Delta k}$	$\frac{\Delta\varepsilon_{\rm GAF}}{(1-n_f)\Delta k}$	$\frac{\Delta\varepsilon_{\rm SBF}}{(1-n_f)\Delta k}$
31	1	0.033	0.203	0.035 ± 0.005	5.22	7.75	4
43	1	0.023	0.146	0.017 ± 0.004	5.06	7.82	4
51	1	0.020	0.123	0.012 ± 0.005	4.88	7.85	4
93	7	0.075	0.068	0.076 ± 0.023	14.9	7.44	4

The second clear result concerns the short-range spin correlations in the Gutzwiller wave function. Such correlations were first found by Kaplan *et al.*[15] for the case of a half-filled band in one dimension in the limit $U \to \infty$. We find that they persist, not surprisingly, into the case when $n_f \neq 1$ but $1-n_f \ll 1$. In this case the GAF describes an almost-localized Fermi liquid. Our results then demonstrate explicitly that it is possible to have a Fermi-liquid state with strong spin correlations. Shiba's MC calculations on the 1D Anderson model[17] also showed strong spin correlations among the f electrons, although the exact form was different to ours, because the Bloch states occupied in the hybridized f bands and in the ground state of the single band differ.[29] Our calculations demonstrate that the form of the spin correlations is sensitive to the distribution of occupied Bloch states.

These results have clear implications for the energy balance between the almost-localized or heavy-Fermi-liquid states and the fully localized magnetic or RKKY states. They show that given the right crystal structure, etc., it is possible to form the Fermi liquid with only a small change in spin correlation so the energy balance between the two states is a subtle one. Perhaps the real criterion deciding between these states is determined by how good the spin correlations can be in the Fermi liquid, which, in turn, depends on crystal structure, band filling, etc. This would agree with the recent experiments of Aeppli *et al.*, who find strong spin correlations characterizing the low-temperature Fermi-liquid state in $CeCu_6$ (Ref. 27) and UPt_3 (Ref. 28).

Note added in proof. Very recently, Metzner and Vollhardt (unpublished) developed a diagrammatic technique to calculate the expectation values of diagonal operators in the ground-state Gutzwiller wave function exactly in one dimension. Their result for $n(k)$ agrees well with ours. Gebhardt and Vollhardt (unpublished) applied these techniques to spin-spin, hole-hole, and other correlation functions. Again, the agreement is excellent. We are grateful to these authors for communicating their results before publication.

ACKNOWLEDGMENTS

We are grateful to P. Horsch, W. Hunziker, and B. S. Shastry for stimulating discussions and correspondence on the use of Monte Carlo methods for Gutzwiller wave functions. The support of the Swiss Nationalfonds is gratefully acknowledged.

TABLE III. Results for excited states where an up and a down electron ($N_f=2$) have been excited from the Fermi surface by $\Delta k = 2\pi/L$. Hence, L and N_h are the number of states and holes, $\Delta q_1 = \langle s_i^z s_{i+1}^z \rangle_{\text{ex}} - \langle s_i^z s_{i+1}^z \rangle_{\text{ground}}$. The last column shows $\Delta q_1/(\Delta k)^2$, which is nearly constant in the two cases of finite density of holes (first four rows) and zero density of holes (last four rows).

L	N_h	Δq_1	$\Delta q_1/(\Delta k)^2$
31	1	0.0063±0.0004	0.153
43	1	0.0033±0.0002	0.155
51	1	0.0022±0.0003	0.145
93	7	0.0006±0.0002	0.121
31	0	0.007±0.0002	0.169
43	0	0.0037±0.0004	0.172
51	0	0.0026±0.0003	0.171
93	0	0.0008±0.0003	0.175

APPENDIX

In this appendix we show how we can calculate–with the Vandermonde method—an excited state where an up or down (or both) spin is promoted from the Fermi surface to $k' = k_F + 2\pi/L$. We have to calculate determinants of the form (see Sec. II)

$$D = \begin{vmatrix} 1 & z_1 & z_1^2 & \cdots & z_1^{N_\sigma-2} & z_1^{N_\sigma} \\ 1 & z_2 & z_2^2 & \cdots & z_2^{N_\sigma-2} & z_2^{N_\sigma} \\ 1 & z_{N_\sigma} & z_{N_\sigma}^2 & \cdots & z_{N_\sigma}^{N_\sigma-2} & z_{N_\sigma}^{N_\sigma} \end{vmatrix} .$$

D is a homogeneous polynomial in $z_1 \cdots z_{N_\sigma}$ of degree $(N_\sigma-1)N_\sigma/2+1$. As a polynomial in z_1, it has the zeroes $z_2, \ldots, z_{N_\sigma}$ similar for $z_2, \ldots, z_{N_\sigma}$. That means

$$D = \prod_{\substack{i,j \\ (i<j)}} (z_i - z_j) f(z_1 \cdots z_{N_\sigma}) .$$

Since D is antisymmetric, f must be a symmetric homogeneous polynomial of order 1 in $z_1 \cdots z_{N_\sigma}$, i.e., $f = z_1 + z_2 + \cdots + z_{N_\sigma}$.

---

*Present address: Department of Physics, University of Wisconsin, Madison, WI 53706.

[1]For reviews of heavy-electron metals, see (a) P. A. Lee, T. M. Rice, J. W. Serene, L. J. Sham, and J. W. Wilkins, Comm. Condens. Matt. Phys. XII, 99 (1986); (b) C. M. Varma, Comm. Solid State Phys. XI, 221 (1985); of ^{3}He, see (c) D. Vollhardt, Rev. Mod. Phys. **56**, 99 (1984).

[2]M. C. Gutzwiller, Phys. Rev. Lett. **10**, 159 (1963); Phys. Rev. **134**, A923 (1964); **137**, A1726 (1965).

[3]S. E. Barnes, J. Phys. F **6**, 1375 (1976).

[4]P. Coleman, Phys. Rev. B **29**, 3035 (1984).

[5]N. Read and D. M. Newns, J. Phys. C **16**, 3273 (1983).

[6]N. Read, D. M. Newns, and S. Doniach, Phys. Rev. B **30**, 384 (1984).

[7]P. Coleman, in *Proceedings of the 8th Taniguchi Conference on the Theory of the Valence Fluctuating State, No. 62 of Springer Series in Solid State Science,* edited by T. Kasuya and T. Saso (Springer-Verlag, Berlin, 1985).

[8]O. T. Valls and Z. Tesanovic, Phys. Rev. Lett. **53**, 1497 (1984).

[9]G. Kotliar and A. Ruckenstein, Phys. Rev. Lett. **57**, 1362 (1986).

[10]T. M. Rice and K. Ueda, Phys. Rev. Lett. **55**, 995 (1986); **55**,

2043(E) (1986); Phys. Rev. B **34**, 6420 (1986).
[11]C. Lacroix and M. Cyrot, Phys. Rev. B **20**, 1969 (1979).
[12]H. Razafimandimby, P. Fulde, and J. Keller, Z. Phys. B **54**, 111 (1984).
[13]B. H. Brandow, Phys. Rev. B **33**, 215 (1986).
[14]A. J. Mills and P. A. Lee, Phys. Rev. B **35**, 3394 (1987); A. Auerbach and K. Levin, Phys. Rev. Lett. **57**, 877 (1986); Phys. Rev. B **34**, 3524 (1986).
[15]T. A. Kaplan, P. Horsch, and P. Fulde, Phys. Rev. Lett. **49**, 889 (1982).
[16](a) P. Horsch and T. A. Kaplan, J. Phys. C **16**, L1203 (1983); (b) Bull. Am. Phys. Soc. **30**, 513 (1985).
[17]H. Shiba, J. Phys. Soc. Jpn. **55**, 2765 (1986).
[18]W. F. Brinkman and T. M. Rice, Phys. Rev. B **2**, 4302 (1970).
[19](a) C. Castellani, C. Di Castro, D. Feinberg, and J. Ranninger, Phys. Rev. Lett. **43**, 1957 (1979); (b) J. E. Hirsch, *ibid.* **54**, 1317 (1985); (c) M. Cyrot, Solid State Commun. **60**, 253 (1986).
[20]D. M. Ceperly, G. U. Chester, and M. H. Kalos, Phys. Rev. B **16**, 3081 (1977).
[21]F. J. Dyson, J. Math. Phys. **3**, 166 (1962).
[22]E. H. Lieb and E. Y. Wu, Phys. Rev. Lett. **20**, 1665 (1968).
[23]R. B. Griffiths, Phys. Rev. **133**, A768 (1964).
[24](a) D. J. Klein and W. A. Seitz, Phys. Rev. B **10**, 3217 (1974); (b) G. Beni, T. Holstein, and P. Pincus, Phys. Rev. B **8**, 321 (1973).
[25]H. Shiba, Phys. Rev. B **6**, 930 (1972).
[26]K. Seiler, C. Gros, T. M. Rice, K. Ueda, and W. Vollhardt, J. Low Temp. Phys. **64**, 195 (1986).
[27]G. Aeppli, H. Yoshizawa, Y. Endoh, E. Bucher, J. Hufnagel, Y. Onuki, and T. Komatsubara, Phys. Rev. Lett. **57**, 122 (1986).
[28]G. Aeppli, A. Goldman, G. Shirane, E. Bucher, and M.-Ch. Lux-Steiner, Phys. Rev. Lett. **58**, 808 (1987).
[29]T. M. Rice, C. Gros, R. Joynt, and M. Sigrint, in Proceedings of the Fifth International Conference on Valence Fluctuations, Bangalore, 1987 (unpublished).